

Why Do Class-Dependent Evaluation Effects Occur with Time Series Feature Attributions? A Synthetic Data Investigation

Gregor Baer^{1,2}[0009-0002-9918-1376], Isel Grau^{1,2}[0000-0002-8035-2887], Chao Zhang^{2,3}[0000-0001-9811-1881], and Pieter Van Gorp^{1,2}[0000-0001-5197-3986]

¹ Information Systems, Eindhoven University of Technology, Eindhoven, The Netherlands

² Eindhoven Artificial Intelligence Systems Institute, Eindhoven University of Technology, Eindhoven, The Netherlands

³ Human-Technology Interaction, Eindhoven University of Technology, Eindhoven, The Netherlands

Abstract. Evaluating feature attribution methods represents a critical challenge in explainable AI (XAI), as researchers typically rely on perturbation-based metrics when ground truth is unavailable. However, recent work demonstrates that these evaluation metrics can show different performance across predicted classes within the same dataset. These “class-dependent evaluation effects” raise questions about whether perturbation analysis reliably measures attribution quality, with direct implications for XAI method development and the trustworthiness of evaluation techniques. We investigate under which conditions these class-dependent effects arise by conducting controlled experiments with synthetic time series data where ground truth feature locations are known. We systematically vary feature types and class contrasts across binary classification tasks, then compare perturbation-based degradation scores with ground truth-based precision-recall metrics using multiple attribution methods. Our experiments demonstrate that class-dependent effects emerge with both evaluation approaches even in simple scenarios with temporally localized features, triggered by basic variations in feature amplitude or temporal extent between classes. Most critically, we find that perturbation-based and ground truth metrics frequently yield contradictory assessments of attribution quality across classes, with weak correlations between evaluation approaches. These findings suggest that researchers should interpret perturbation-based metrics with care, as they may not always align with whether attributions correctly identify discriminating features. These findings reveal opportunities to reconsider what attribution evaluation actually measures and to develop more comprehensive evaluation frameworks that capture multiple dimensions of attribution quality.

Keywords: Feature attribution · Perturbation analysis · XAI evaluation · Time series classification.

1 Introduction

As machine learning models of increasing complexity advance prediction accuracy across domains, including time series classification [7], the field of Explainable Artificial Intelligence (XAI) has emerged to answer why models make certain predictions. However, a fundamental challenge in XAI research continues to be the evaluation of explanations. It remains challenging to determine what makes an explanation “good” and how to best evaluate explanation quality without ground truth labels, unlike prediction tasks where true outcomes enable direct performance measurement.

While human-centered evaluation through user studies provides direct assessment of explanation utility [10], such approaches demand substantial time and resources, limiting their use during XAI method development. Consequently, XAI researchers frequently employ functional evaluation techniques that computationally verify whether explanations satisfy desirable properties [2,8]. This computational approach enables quicker iteration and systematic comparison across methods, making it essential for advancing XAI research.

Researchers have adapted feature attribution methods originally developed for images to time series classification and evaluated them functionally, including [12,16,13,21,9,15]. These evaluations predominantly rely on perturbation analysis, first introduced by Samek et al. [11], which operates under the assumption that modifying features identified as important should proportionally degrade model output. This approach has become the de facto standard for attribution evaluation in the absence of ground truth.

However, Baer et al. [1] recently identified a potential methodological limitation: “class-dependent perturbation effects”, where perturbation-based metrics demonstrate different performance across predicted classes within datasets. This phenomenon creates a problem because benchmarks relying on average scores can mask class-specific biases, potentially leading researchers to incorrect conclusions about attribution method quality. Although previous research acknowledges that perturbation results vary by perturbation strategy and recommends testing multiple approaches [16,13], class-dependent effects seem to persist across various perturbation methods and datasets [1]. The conditions generating these effects remain unexplored, leaving a gap in our understanding of how to reliably evaluate feature attributions.

Understanding why these effects arise carries critical implications for XAI evaluation methodology. If class-dependent differences reflect genuine variations in attribution quality, where methods truly perform better for certain classes, then perturbation analysis correctly captures these differences. However, if perturbation analysis itself introduces systematic biases regardless of attribution quality, researchers may draw misleading conclusions about method performance. This distinction fundamentally affects how we interpret and trust XAI evaluation results.

Our research addresses this gap by investigating: **Under which conditions do class-dependent evaluation effects arise?** We approach this question through systematically constructed synthetic data experiments, creating binary

time series classification tasks with known ground truth features localized in time. By varying feature types (level shifts, pulses, sine waves, trends) and class contrasts (amplitude, length), we isolate factors contributing to evaluation disparities.

This paper offers three primary contributions to XAI evaluation methodology. First, we identify specific conditions under which class-dependent evaluation differences emerge, demonstrating that these effects manifest even in minimally complex classification tasks. We show that simple variations in feature prevalence and amplitude across classes trigger class-dependent effects, even when the underlying discriminating feature remains structurally identical between classes. Second, we reveal that class-dependent effects occur in both ground truth-based and perturbation-based evaluation metrics, indicating that attribution methods genuinely perform differently across classes rather than reflecting measurement artifacts. Third, and most critically, we demonstrate that ground truth and perturbation metrics can yield contradictory assessments of attribution quality across classes, revealing that these approaches may measure fundamentally different aspects of attribution behavior. While ground truth metrics assess whether attributions locate discriminating features, perturbation analysis may capture other properties that do not necessarily align with feature identification accuracy. By showing when and why evaluation metrics diverge, our work advances efforts toward more rigorous assessment frameworks in time series analysis as advocated by Theissler et al. [20].

The remainder of this paper is organized as follows. Section 2 establishes our evaluation framework, including perturbation-based and ground truth-based metrics with synthetic data generation. Section 3 details our experimental design across different feature types, class contrasts, and attribution methods. Section 4 presents findings on when class-dependent evaluation effects emerge and analyzes the correspondence between evaluation approaches. Section 5 summarizes our contributions and implications for XAI evaluation methodology.

2 Evaluation Framework

Feature attribution methods for time series classification identify the time points that influence a model’s predictions. Since ground truth is typically unavailable for real-world data, perturbation analysis is commonly used to assess attribution quality by modifying input features and observing the impact on model predictions. The underlying assumption is that perturbing important time points should cause significant prediction changes, while modifying irrelevant time points should have minimal impact. In this work, we evaluate feature attributions using both perturbation-based metrics and ground truth comparison on synthetic data where true feature locations are known. See also Figure 1 for an overview of the evaluation framework.

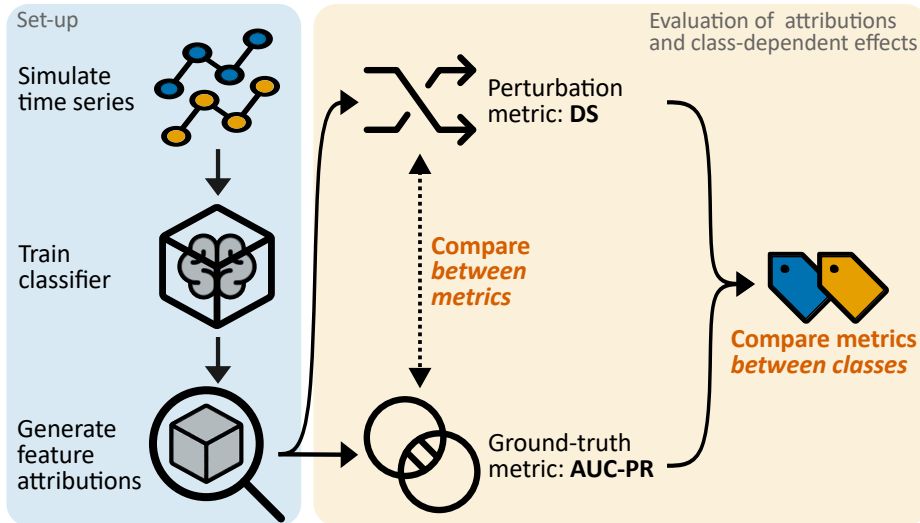


Fig. 1: Framework for analyzing class-dependent evaluation effects. We generate synthetic time series with features localized in time, train classifiers, and compare perturbation-based versus ground truth-based attribution evaluations to identify when class-dependent evaluation effects arise.

2.1 Perturbation-Based Attribution Evaluation

We use the degradation score (DS) for perturbation analysis, following the approach of Baer et al [1]. The DS, originally introduced by Schulz et al. [14] and first applied to time series by Šimić et al. [16], compares attribution quality by contrasting two perturbation sequences: most relevant features first (MoRF) versus least relevant features first (LeRF).

Consider a univariate time series $\mathbf{x} = [x_1, \dots, x_N]$ where a trained classifier $f(\mathbf{x})$ generates class probability distributions with q_c representing the confidence for class c . We evaluate feature attribution methods that produce temporal importance scores $\mathbf{r} = [r_1, \dots, r_N]$, where higher values of r_i indicate greater relevance of timestep i for the classifier’s decision.

We perturb \mathbf{x} by replacing timestep values with zero ($x'_i = 0$) or Gaussian noise ($x'_i \sim \mathcal{N}(0, 1)$), creating two perturbation sequences: MoRF perturbs timesteps in descending order of attribution scores, while LeRF perturbs in ascending order. The DS compares these sequences:

$$\text{DS} = \frac{1}{m} \sum_i^m (\text{PC}_{\text{LeRF}_i} - \text{PC}_{\text{MoRF}_i}), \quad (1)$$

where $\text{PC}_{\text{order}_i}$ represents the predicted probabilities after perturbing i features in the specified order. The DS ranges from -1 to 1, with positive values indicating effective attributions, i.e. MoRF perturbations degrade predictions more than LeRF.

2.2 Synthetic Data Generation

In addition to perturbation analysis, we construct synthetic time series data with known ground truth feature locations to directly evaluate attribution correctness. This allows us to assess whether attribution methods can correctly identify the specific time points where class-discriminating features are located.

Each synthetic time series \mathbf{x} contains a single class-discriminating, contiguous feature over multiple time points embedded within a foundation signal through additive composition:

$$\mathbf{x} = \mathbf{n} + \mathbf{f}, \quad (2)$$

where $\mathbf{n} \sim \mathcal{N}(0, 1)$ represents background noise and \mathbf{f} contains the class-specific temporal pattern within a designated feature window, with zeros elsewhere. Both vectors have identical length to enable element-wise addition.

While real-world time series features may exhibit complex temporal dependencies, we deliberately restrict investigation to temporally localized features occupying contiguous windows of predetermined length L . This design choice isolates evaluation effects under minimal complexity conditions, enabling attribution of observed phenomena to specific data characteristics rather than confounding factors. Class-dependent variations are introduced through two systematic contrast mechanisms. *Feature length contrast* varies temporal extent between classes, testing whether feature prevalence affects evaluation metrics. *Amplitude contrast* varies signal magnitude between classes, examining whether signal strength differences drive evaluation disparities. Feature locations are randomized across observations to prevent positional classification shortcuts. For an example of this approach, see Figure 2, which shows two possible instances with different classes from a simulated dataset.

2.3 Ground Truth-Based Attribution Evaluation

To evaluate feature attributions on synthetic data, we treat attribution evaluation as a retrieval problem: can high attribution scores identify true feature locations? Let $\mathbf{l} = [l_1, \dots, l_N]$ where $l_i \in \{0, 1\}$ represent a binary mask indicating ground truth feature locations, with $l_i = 1$ denoting the presence of a class-discriminating feature f_i at time point i . For attribution scores \mathbf{r} , we threshold at different values t to obtain binary predictions $\hat{l}_i^{(t)} = I(r_i \geq t)$ of important feature locations. We use all unique attribution values as thresholds, evaluated in descending order, which ensures we capture all possible precision-recall operating points. At each threshold, we compute:

$$\text{Precision}(t) = \frac{TP(t)}{TP(t) + FP(t)}, \quad \text{Recall}(t) = \frac{TP(t)}{P}, \quad (3)$$

where $TP(t) = \sum_{i=1}^N \hat{l}_i^{(t)} \cdot l_i$ (correctly identified feature locations), $FP(t) = \sum_{i=1}^N \hat{l}_i^{(t)} \cdot (1 - l_i)$ (false feature locations), and $P = \sum_{i=1}^N l_i$ (total ground truth features).

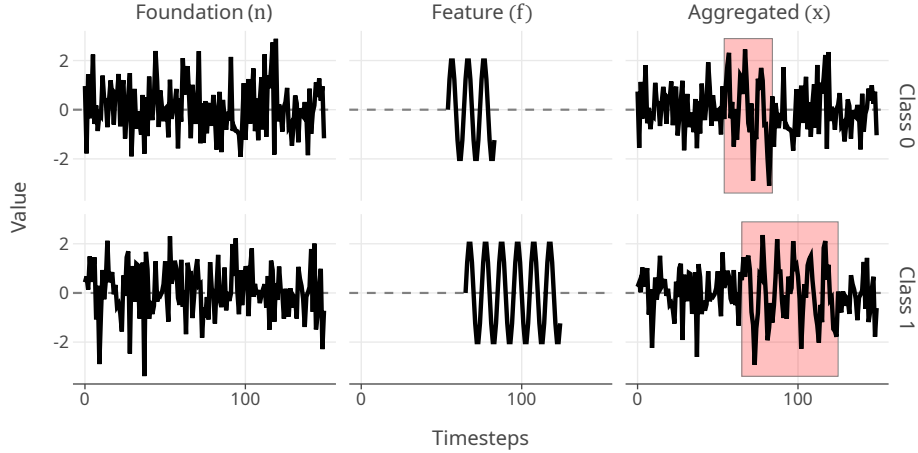


Fig. 2: Synthetic data generation example demonstrating feature length contrast. Two instances show identical sine wave features (red regions) with different temporal extents: Class 0 spans 20% of timesteps while Class 1 spans 40%.

To assess whether feature attributions correctly highlight crucial regions within the time series, we compute the AUC-PR. This metric calculates the area beneath the precision-recall curve, where precision is plotted as a function of recall:

$$\text{AUC-PR} = \int_0^1 \text{Precision}(\text{recall}) d(\text{recall}), \quad (4)$$

computed using the trapezoidal rule over unique recall values. We choose AUC-PR because it suits our sparse ground truth features well. For binary classification problems, the random baseline equals the feature prevalence $\text{Prevalence} = \frac{P}{N}$ rather than 0.5.

Since we vary feature lengths across experiments, we normalize the AUC-PR to enable fair comparison across different prevalence rates:

$$\text{AUC-PR}' = \frac{\text{AUC-PR} - \text{Prevalence}}{1 - \text{Prevalence}}. \quad (5)$$

This normalized score represents improvement over the random baseline, with values approaching 1 indicating perfect performance and negative values indicating worse-than-random attribution quality.

3 Experimental Design

Dataset specifications. We construct synthetic datasets consisting of univariate time series with 150 timesteps for binary classification tasks. Each dataset comprises 1000 training samples, 300 validation samples, and 300 test samples

with balanced class distributions. While all sets are generated from the same data-generating process, we use different random seeds to ensure independence. Class-discriminating features are randomly positioned within each time series, with feature windows $[t_{\text{start}}, t_{\text{start}} + L - 1]$ varying across observations to prevent positional classification shortcuts. All instances undergo standardization prior to model training.

Feature types. We implement four feature types to represent common temporal patterns: (1) level shifts representing constant amplitude changes, (2) Gaussian pulses capturing transient spikes, (3) sine waves modeling periodic oscillations reminiscent of seasonality, and (4) local trends reflecting gradual directional changes. Definitions and parameters for each feature type are provided in Table 1.

Table 1: Feature type definitions. Formulas show signal generation within the feature window, where $t \in [0, L - 1]$ is the relative timestep. Parameters: $A =$ amplitude, $L =$ feature window length, $p =$ period, $\sigma = L/6 =$ pulse width.

Feature	Shape	Description	Definition
Level		Constant amplitude/level shift	$f(t) = A$
Pulse		Gaussian-shaped transient signal	$f(t) = Ae^{-\frac{(t-L/2)^2}{2\sigma^2}}$, $\sigma = L/6$
Sine		Periodic oscillation	$f(t) = A \sin(2\pi t/p)$, $p = 10$
Trend		Linear increase from zero	$f(t) = At/(L - 1)$

Class contrasts. We create binary classification tasks by systematically contrasting features across two dimensions: amplitude differences to examine magnitude-based discrimination, and length differences to investigate temporal prevalence effects. This design isolates how different types of class distinctions influence attribution evaluation metrics. We embed features within background Gaussian noise, with feature amplitudes chosen to maintain detectability while avoiding trivial separability. Feature lengths span 20% to 40% of the time series to represent moderate temporal prevalence. Combining four feature types with two contrast mechanisms yields eight datasets. Table 2 summarizes the specific class differences for each contrast type. For example, amplitude-contrast datasets vary only feature magnitude while maintaining identical temporal extent, whereas length-contrast datasets vary temporal coverage while preserving signal strength.

Model architecture and training. We employ two established deep learning architectures for time series classification: ResNet [22] and InceptionTime [6], both of which offer robust performance across time series benchmarks [3]. We train models using AdamW optimization with cosine annealing learning rate scheduling

Table 2: Experimental class contrasts applied to all four feature types (Level, Pulse, Sine, Trend; see Table 1). Parameters: A = feature amplitude, L = feature window length (timesteps), \mathbf{n} = background noise.

Contrast	Class 0	Class 1	Both classes	Purpose
Amplitude	$A = 1$	$A = 2$	$\mathbf{n} \sim \mathcal{N}(0, 1), L = 60$	Test magnitude effects
Length	$L = 30$	$L = 60$	$\mathbf{n} \sim \mathcal{N}(0, 1), A = 2$	Test prevalence effects

and early stopping (patience = 10 epochs) based on validation performance over a maximum of 100 epochs. Both architectures achieve test accuracy and weighted F1 scores exceeding 0.9 across all datasets, with one exception: InceptionTime on the Amplitude-Pulse dataset (F1 = 0.7). These performance levels ensure that observed class-dependent evaluation differences stem from attribution or perturbation methodology rather than classifier bias toward specific classes. Complete performance metrics are provided in Table 3 (Appendix A).

Attribution methods. We evaluate three attribution methods: Gradients (GR) [17], Integrated Gradients (IG) [19], and Feature Occlusion (FO) [4]. IG and FO were selected because they demonstrated both high attribution quality and pronounced class-dependent evaluation effects in previous research [1], making them suitable candidates for investigating the conditions under which such effects arise. We include GR as a computationally efficient baseline to ensure our findings span different levels of attribution complexity. The selection covers both gradient-based approaches (GR and IG) and perturbation-based attribution (FO). We compute attributions for all 300 test samples, explaining each model’s predicted class label.

Perturbation analysis. We employ two perturbation strategies: replacing values with zero and substituting with Gaussian noise. Both strategies are commonly used in time series attribution evaluation [13,16,21]. Since we standardize all time series, zero substitution effectively replaces values with the sample mean. For Gaussian noise perturbation, we sample from the same distribution as the background noise ($\mathcal{N}(0, 1)$), following the controlled masking approach used in existing benchmarks [5]. This approach ensures that perturbations align more closely with the data distribution, avoiding the potential artifacts of more extreme substitution methods or constant replacement values. We implement perturbation according to MoRF and LeRF orderings determined by attribution scores, substituting features incrementally one timestep at a time. To maintain fair comparisons across datasets with varying feature lengths, we perturb exactly L timesteps for each sample, where L corresponds to the true feature window size. For instance, in length-contrast datasets, we perturb 30 timesteps for class 0 samples and 60 timesteps for class 1 samples. We record predicted probabilities after each perturbation step to calculate the DS.

4 Results and Discussion

Figure 3 presents the AUC-PR' and DS across datasets and true class labels (detailed results for all experimental conditions appear in Appendix A). We aggregate results across attribution methods and model architectures to emphasize general patterns in class-dependent evaluation effects, though individual method-specific variations exist within these trends.

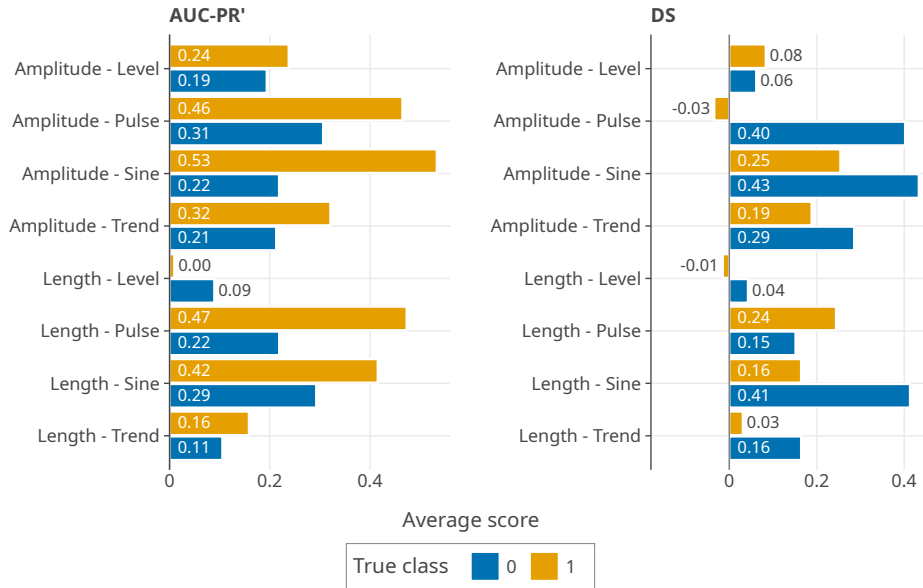


Fig. 3: Average AUC-PR' and DS by dataset and true class.

Ground truth-based evaluation. The ground truth evaluation reveals substantial variation in how well attribution methods recover true class-discriminating feature regions, both across datasets and between classes within datasets. Class 1 observations (with higher amplitude or longer feature windows) consistently achieve higher AUC-PR' scores than class 0 observations across seven of eight datasets. The Length-Level dataset is the sole exception where class 1 attributions approach random performance. Overall, Pulse, Sine, and Trend features demonstrate pronounced class-dependent differences in attribution quality. The disparities prove particularly large for Amplitude-Sine and Length-Pulse datasets: class 1 observations in both achieve AUC-PR' scores more than double those of class 0 observations, indicating that attribution methods recover ground truth features far more effectively for one class than the other.

Perturbation-based evaluation. Perturbation-based evaluation through DS scores reveals patterns that directly contradict the ground truth findings. Ground truth-based evaluation favors class 1 attributions in seven of eight

datasets, while perturbation analysis indicates better attribution quality for class 0 observations in six of eight datasets. This systematic reversal across most feature types and contrast mechanisms suggests the two evaluation approaches measure fundamentally different aspects of attribution behavior. Only two datasets show convergence between evaluation approaches. Both Length-Level and Amplitude-Level datasets exhibit minimal class discrepancies, with both metrics assigning relatively low scores that reflect the sparse attribution patterns characteristic of level shift detection. Only two datasets demonstrate consistent patterns across evaluation approaches. Both Length-Level and Amplitude-Level datasets show smaller class discrepancies within their respective metrics, with both approaches assigning relatively low scores. These lower scores may reflect how attribution methods concentrate on temporal change points rather than extended feature windows when detecting level shifts. This localized attribution behavior could reduce overlap with our ground truth evaluation windows and limit perturbation impact when removing individual timesteps within the feature region. Interestingly, datasets that achieve the highest scores for one class also exhibit the most pronounced disagreement about which class receives superior attribution quality. This pattern appears in both ground truth and perturbation-based evaluation, demonstrating the tension between evaluation approaches even when overall performance appears strong.

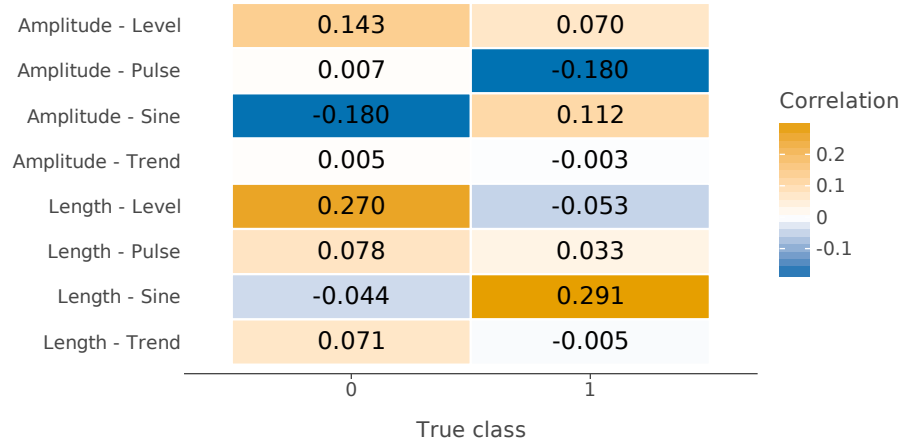


Fig. 4: Average Spearman correlation between $\text{AUC-PR}'$ and DS by dataset and true class. Correlations are computed per observation, then averaged.

Correspondence between evaluation approaches. To examine the relationship between evaluation approaches, we compute Spearman correlations between $\text{AUC-PR}'$ and DS scores. We use Spearman correlation because the metrics operate on different scales and we focus on monotonic relationships, that is, whether higher scores in one metric correspond to higher scores in the other.

Figure 4 shows correlations between both metrics per dataset and class. The analysis confirms our earlier observations about contradictory class-dependent evaluation effects. Correlations remain weak to moderate, ranging from -0.18 to 0.291, and vary substantially between classes within datasets. For example, Amplitude-Sine shows a negative correlation (-0.18) for class 0 but a positive correlation (0.112) for class 1. Similarly, Length-Sine achieves the highest correlation (0.291) for class 1 while class 0 shows a slight negative correlation. These results demonstrate that perturbation-based and ground truth metrics seem to provide different assessments of attribution quality. The weak correspondence indicates that perturbation analysis does not reliably identify whether feature attributions correctly locate true class-discriminating regions in our experimental settings.

Summary. Class-dependent evaluation differences emerge across almost all feature types and contrast mechanisms. Ground truth and perturbation-based metrics yield contradictory assessments: while ground truth evaluation favors class 1 attributions in seven of eight datasets, perturbation analysis indicates better performance for class 0 in six of eight cases. Correlations between approaches remain weak and inconsistent, ranging from -0.18 to 0.291 across datasets and classes.

5 Conclusion

We investigate conditions under which class-dependent evaluation effects arise in time series feature attribution assessment. Through controlled synthetic experiments with known ground truth features, we compare perturbation-based and ground truth-based evaluation metrics across multiple attribution methods. Our results demonstrate that even simple variations in feature characteristics, such as amplitude differences or temporal extent, can trigger pronounced evaluation disparities between classes. These class-dependent effects emerge consistently across feature types and contrast mechanisms. Most notably, the two evaluation approaches often disagree: perturbation-based metrics frequently suggest superior attribution quality for one class while ground truth metrics indicate the opposite.

These findings highlight important considerations for XAI evaluation in time series domains. While perturbation-based evaluation remains valuable when ground truth is unavailable, our results suggest researchers should interpret such metrics cautiously, recognizing they may not reflect whether attributions correctly identify discriminating features. When synthetic or annotated data permit ground truth comparison, using both evaluation approaches reveals potential contradictions rather than providing validation, as demonstrated in our experimental conditions. We believe that such challenges likely persist and may even compound in more realistic time series datasets.

Our deliberate focus on simplified synthetic scenarios with temporally localized features successfully isolates some of the conditions under which class-dependent effects can emerge, demonstrating that these evaluation challenges arise even under minimal complexity. However, several limitations constrain the generalizability of our findings. We examine only simple univariate time series with

temporally localized features, employing two deep learning architectures and three general-purpose attribution methods. While this design enables controlled analysis, it excludes complex temporal patterns and specialized attribution approaches designed for time series. Our evaluation also assumes that good attributions should cover entire feature windows, yet models may legitimately focus on sparse temporal markers like change points. When models identify features through different strategies than we expect, standard metrics may underestimate their actual attribution quality. This mismatch between how we measure attribution performance and how models process temporal information highlights the challenge of defining “correct” attributions in time series contexts.

Future research can address both empirical and conceptual dimensions of these evaluation challenges. Testing time series-specific attribution methods like Lime-Segment [18] may reveal whether specialized approaches reduce class-dependent effects. Expanding synthetic datasets to include multiple discriminating patterns and more complex temporal dependencies would test generalizability beyond our localized feature settings. More fundamentally, the weak correspondence between perturbation and ground truth metrics highlights the need to reconsider what attribution evaluation actually measures. For instance, when models correctly identify temporal change points but evaluation metrics expect coverage of entire feature windows, apparent “poor performance” may actually reflect misaligned measurement assumptions. These insights point toward developing evaluation frameworks that embrace multiple perspectives on attribution quality, moving beyond single-metric assessments to better understand how models process temporal information.

A Detailed Experimental Results

Table 3: Model performance by dataset on the test set.

Contrast	Feature	ResNet		InceptionTime	
		Accuracy	F1	Accuracy	F1
Amplitude	Level	0.990	0.990	0.980	0.980
	Pulse	0.900	0.899	0.723	0.700
	Sine	0.997	0.997	1.000	1.000
	Trend	0.920	0.920	0.940	0.940
Length	Level	1.000	1.000	1.000	1.000
	Pulse	0.923	0.923	0.947	0.947
	Sine	0.997	0.997	1.000	1.000
	Trend	0.927	0.927	0.973	0.973

Table 4: Average AUC-PR' by classifier, dataset, attribution method and true class.

Model	Contrast	Feature	GR		IG		FO	
			C0	C1	C0	C1	C0	C1
ResNet	Amplitude	Level	.134	.234	.435	.384	-.032	-.068
		Pulse	.235	.313	.188	.284	.151	.270
		Sine	.219	.357	.170	.262	.308	.681
		Trend	.126	.127	.074	.278	.058	.058
	Length	Level	.190	.483	.038	-.101	.102	-.038
		Pulse	.179	.329	.226	.313	.158	.197
		Sine	.262	.358	.139	.166	.304	.455
		Trend	.004	.129	-.018	-.024	-.004	-.013
InceptionTime	Amplitude	Level	.280	.503	.275	.225	.071	.148
		Pulse	.574	.750	.264	.572	.427	.599
		Sine	.139	.573	.256	.645	.219	.681
		Trend	.345	.528	.451	.588	.223	.348
	Length	Level	.033	-.002	.147	-.101	.025	-.183
		Pulse	.274	.733	.248	.711	.226	.555
		Sine	.226	.300	.512	.684	.312	.528
		Trend	.285	.386	.208	.306	.158	.166

Table 5: Average DS by classifier, dataset, perturbation strategy, attribution method, and true class.

Model	Contrast	Feature	Perturbation	GR		IG		FO	
				C0	C1	C0	C1	C0	C1
ResNet	Amplitude	Level	Gaussian	.133	-.460	.023	.185	-.001	.054
			Zero	.155	-.430	-.027	.508	.013	.043
		Pulse	Gaussian	.510	-.296	.543	-.093	.340	.042
			Zero	.639	-.220	.712	-.026	.480	.086
		Sine	Gaussian	.266	.083	.551	-.072	.334	.229
			Zero	.511	.043	.778	-.067	.561	.231
		Trend	Gaussian	.474	-.204	.391	-.020	.286	.057
			Zero	.634	-.199	.446	.051	.336	.085
	Length	Level	Gaussian	.116	-.142	.010	-.071	-.029	.032
			Zero	.090	-.140	.016	.081	.004	.171
		Pulse	Gaussian	.314	-.179	.146	.086	.150	.062
			Zero	.283	-.140	.078	.353	.111	.246
		Sine	Gaussian	.439	-.066	.505	-.030	.399	.074
			Zero	.677	-.023	.737	-.029	.621	.019
		Trend	Gaussian	.378	-.291	.116	-.099	.179	-.069
			Zero	.347	-.353	-.020	.204	.034	.158
InceptionTime	Amplitude	Level	Gaussian	.187	-.157	.120	.114	.049	.187
			Zero	.089	.049	-.006	.449	.005	.459
		Pulse	Gaussian	.390	-.191	.169	-.095	.263	-.122
			Zero	.420	.124	.089	.252	.268	.129
		Sine	Gaussian	.230	.458	.383	.412	.261	.434
			Zero	.371	.453	.537	.415	.417	.428
	Trend	Gaussian	.256	.112	.181	.331	.199	.273	
		Zero	.207	.426	-.011	.718	.027	.627	
	Length	Level	Gaussian	.032	-.058	.110	-.078	.021	-.060
			Zero	.017	-.116	.115	.038	.009	.164
		Pulse	Gaussian	.179	.273	.112	.351	.167	.291
			Zero	.152	.508	.021	.538	.105	.540
Sine		Gaussian	.178	.242	.227	.456	.206	.428	
		Zero	.293	.150	.347	.387	.330	.362	
Trend	Gaussian	.162	-.087	.259	.135	.210	.101		
	Zero	.093	.021	.066	.404	.145	.245		

Acknowledgments. This paper is supported by the European Union’s HORIZON Research and Innovation Program under grant agreement No. 101120657, project ENFIELD (European Lighthouse to Manifest Trustworthy and Green AI).

Disclosure of Interests. All authors declare that they have no conflicts of interest.

References

1. Baer, G., Grau, I., Zhang, C., Van Gorp, P.: Class-dependent perturbation effects in evaluating time series attributions. In: Proceedings of the 3rd World Conference on eXplainable Artificial Intelligence (XAI-2025) (2025), in Press. Preprint available: arXiv:2502.17022
2. Doshi-Velez, F., Kim, B.: Considerations for Evaluation and Generalization in Interpretable Machine Learning. In: Escalante, H.J., Escalera, S., Guyon, I., Baró, X., Güçlütürk, Y., Güçlü, U., van Gerven, M. (eds.) Explainable and Interpretable Models in Computer Vision and Machine Learning, pp. 3–17. Springer (2018). https://doi.org/10.1007/978-3-319-98131-4_1
3. Fawaz, H.I., Forestier, G., Weber, J., Idoumghar, L., Muller, P.A.: Deep learning for time series classification: A review. *Data Mining and Knowledge Discovery* **33**, 917–963 (2019). <https://doi.org/10.1007/s10618-019-00619-1>
4. Fong, R.C., Vedaldi, A.: Interpretable Explanations of Black Boxes by Meaningful Perturbation. In: Proceedings of the IEEE International Conference on Computer Vision. pp. 3429–3437 (2017), https://openaccess.thecvf.com/content_iccv_2017/html/Fong_Interpretable_Explanations_of_ICCV_2017_paper.html
5. Ismail, A.A., Gunady, M., Corrada Bravo, H., Feizi, S.: Benchmarking deep learning interpretability in time series predictions. *Advances in neural information processing systems* **33**, 6441–6452 (2020), https://proceedings.neurips.cc/paper_files/paper/2020/hash/47a3893cc405396a5c30d91320572d6d-Abstract.html
6. Ismail Fawaz, H., Lucas, B., Forestier, G., Pelletier, C., Schmidt, D.F., Weber, J., Webb, G.I., Idoumghar, L., Muller, P.A., Petitjean, F.: InceptionTime: Finding AlexNet for time series classification. *Data Mining and Knowledge Discovery* **34**, 1936–1962 (2020). <https://doi.org/10.1007/s10618-020-00710-y>
7. Middlehurst, M., Schäfer, P., Bagnall, A.: Bake off redux: A review and experimental evaluation of recent time series classification algorithms. *Data Mining and Knowledge Discovery* **38**, 1958–2031 (2024). <https://doi.org/10.1007/s10618-024-01022-1>
8. Nauta, M., Trienes, J., Pathak, S., Nguyen, E., Peters, M., Schmitt, Y., Schlötterer, J., Van Keulen, M., Seifert, C.: From Anecdotal Evidence to Quantitative Evaluation Methods: A Systematic Review on Evaluating Explainable AI. *ACM Computing Surveys* **55**, 1–42 (2023). <https://doi.org/10.1145/3583558>
9. Nguyen, T.T., Le Nguyen, T., Ifrim, G.: Robust explainer recommendation for time series classification. *Data Mining and Knowledge Discovery* **38**, 3372–3413 (2024). <https://doi.org/10.1007/s10618-024-01045-8>
10. Rong, Y., Leemann, T., Nguyen, T.T., Fiedler, L., Qian, P., Unhelkar, V., Seidel, T., Kasneci, G., Kasneci, E.: Towards Human-Centered Explainable AI: A Survey of User Studies for Model Explanations. *IEEE Transactions on Pattern Analysis and Machine Intelligence* **46**, 2104–2122 (2024). <https://doi.org/10.1109/TPAMI.2023.3331846>
11. Samek, W., Binder, A., Montavon, G., Lapuschkin, S., Müller, K.R.: Evaluating the Visualization of What a Deep Neural Network Has Learned. *IEEE Transactions*

- on Neural Networks and Learning Systems **28**, 2660–2673 (2017). <https://doi.org/10.1109/TNNLS.2016.2599820>
12. Schlegel, U., Arnout, H., El-Assady, M., Oelke, D., Keim, D.A.: Towards a rigorous evaluation of XAI methods on time series. In: 2019 IEEE/CVF International Conference on Computer Vision Workshop (ICCVW). pp. 4197–4201 (2019). <https://doi.org/10.1109/ICCVW.2019.00516>
 13. Schlegel, U., Keim, D.A.: A Deep Dive into Perturbations as Evaluation Technique for Time Series XAI. In: Longo, L. (ed.) Explainable Artificial Intelligence, vol. 1903, pp. 165–180. Springer Nature Switzerland, Cham (2023). https://doi.org/10.1007/978-3-031-44070-0_9
 14. Schulz, K., Sixt, L., Tombari, F., Landgraf, T.: Restricting the flow: Information bottlenecks for attribution. In: International Conference on Learning Representations (2020), <https://openreview.net/forum?id=S1xWh1rYwB>
 15. Serramazza, D.I., Nguyen, T.L., Ifrim, G.: Improving the Evaluation and Actionability of Explanation Methods for Multivariate Time Series Classification. In: Bifet, A., Davis, J., Krilavičius, T., Kull, M., Ntoutsis, E., Žliobaitė, I. (eds.) Machine Learning and Knowledge Discovery in Databases. Research Track. pp. 177–195 (2024). https://doi.org/10.1007/978-3-031-70359-1_11
 16. Simić, I., Sabol, V., Veas, E.: Perturbation effect: A metric to counter misleading validation of feature attribution. In: Proceedings of the 31st ACM International Conference on Information & Knowledge Management. pp. 1798–1807 (2022). <https://doi.org/10.1145/3511808.3557418>
 17. Simonyan, K., Vedaldi, A., Zisserman, A.: Deep inside convolutional networks: Visualising image classification models and saliency maps. In: Proceedings of the International Conference on Learning Representations (ICLR) (2014). <https://doi.org/10.48550/arXiv.1312.6034>
 18. Sivill, T., Flach, P.: LIMESegment: Meaningful, Realistic Time Series Explanations. In: Proceedings of The 25th International Conference on Artificial Intelligence and Statistics. pp. 3418–3433 (2022), <https://proceedings.mlr.press/v151/sivill22a.html>
 19. Sundararajan, M., Taly, A., Yan, Q.: Axiomatic Attribution for Deep Networks. In: Proceedings of the 34th International Conference on Machine Learning. pp. 3319–3328 (2017), <https://proceedings.mlr.press/v70/sundararajan17a.html>
 20. Theissler, A., Spinnato, F., Schlegel, U., Guidotti, R.: Explainable AI for Time Series Classification: A Review, Taxonomy and Research Directions. IEEE Access **10**, 100700–100724 (2022). <https://doi.org/10.1109/ACCESS.2022.3207765>
 21. Turbé, H., Bjelogrić, M., Lovis, C., Mengaldo, G.: Evaluation of post-hoc interpretability methods in time-series classification. Nature Machine Intelligence **5**, 250–260 (2023). <https://doi.org/10.1038/s42256-023-00620-w>
 22. Wang, Z., Yan, W., Oates, T.: Time series classification from scratch with deep neural networks: A strong baseline. In: 2017 International Joint Conference on Neural Networks (IJCNN). pp. 1578–1585 (2017). <https://doi.org/10.1109/IJCNN.2017.7966039>